MicroRNA-223-3p attenuates the angiotensin II-dependent ROS effect on cell viability by targeting NLRP3 in H9c2 cells

Weiran Dai, Shuang Zhou, Zhiyuan Jiang, Guoqiang Zhong

Department of Cardiology, the First Affiliated Hospital of Guangxi Medical University, Guangxi Cardiovascular Institute, Nanning, Guangxi, China

Submitted: 18 December 2019; **Accepted:** 4 March 2020
Online publication: 28 March 2021

Arch Med Sci
DOI: https://doi.org/10.5114/aoms/118738

Corresponding author:
Guoqiang Zhong PhD
Department of Cardiology
The First Affiliated Hospital of Guangxi Medical University
Guangxi Cardiovascular Institute, Nanning
Guangxi 530021, China
E-mail: drguoqiang@sina.com

Abstract

Introduction: Recently, enhanced activation of NLRP3 has been reported to be involved in atrial fibrillation (AF). This study aimed to detect the correlation between oxidative stress and NLRP3 and explore the role of miR-223-3p in the reactive oxygen species (ROS) injury induced by Ang II.
Material and methods: Serum Ang II levels were examined using an ELISA kit. Fibrosis levels of right atrial appendages were determined by Masson's staining. H9c2 cells transfected with miR-223-3p mimics were treated with Ang II with or without MCC950 (a potent selective NLRP3 inhibitor). Cell viability was detected by CCK-8 assay. Protein abundance was detected by Western blot. The malondialdehyde assay and DCFH-DA were used to measure oxidative stress. RT-qPCR was used to assay the expression of miR-223-3p and NLRP3.
Results: In total, 43 patients enrolled in this study, including 20 patients with persistent (chronic) AF (cAF). Compared with the sinus rhythm (SR) group, we found enhanced activation of the NLRP3 inflammasome which was positively correlated with oxidative stress and serum Ang II level in cAF patients. Ang II induced ROS generation and inhibited H9c2 cell viability. In addition, overexpression of miR-223-3p functioned as MCC950 which inhibited expression of the NLRP3 inflammasome and partly attenuated the effects of ROS induced by Ang II on H9c2 cell viability. Lastly, we used luciferase assay to confirm NLRP3 as a direct target gene of miR-223-3p.
Conclusions: miR-223-3p has protective effects on oxidative stress induced by Ang II in AF by targeting NLRP3 and could provide a new potential intervention target for treatment of AF.

Key words: miR-223-3p, NLRP3, oxidative stress, atrial fibrillation.

Introduction

Atrial fibrillation (AF) is a common tachyarrhythmia, which is characterized by a high risk of stroke, heart failure and mortality [1]. More than 30 million people worldwide suffer from AF, with an average incidence of about 3% [2]. A recent survey of current conditions found that there are about 4.87 million patients with AF over the age of 35 in China.

At present, the pathogenesis of AF is not completely known. The enhanced activation of nucleotide-binding oligomerization domain-like receptor protein 3 (NLRP3) inflammasome and oxidative stress may be two potential mechanisms leading to AF. The NLRP3 inflammasome plays an

important role in pyroptosis. Pyroptosis is a novel type of caspase 1- dependent programmed cell death caused by activated inflammasomes. It has been found to be involved in different cellular processes in various diseases, including renal ischemia reperfusion injury, diabetic nephropathy, nerve injury and atherosclerosis [3–5]. The activated NLRP3 inflammasomes induce pro-caspase-1, which upon maturation subsequently releases inflammatory cytokines leading to pyroptosis [6]. However, only a few studies have been conducted on the role of NLRP3 in the occurrence and maintenance of AF. In one of our previous studies, we found an increase in the expression of NLRP3 and IL-1β in the peripheral blood mononuclear cells (PBMCs) of AF patients, suggesting that NLRP3 inflammasome signaling had a role in AF [7]. Nevertheless, the specific molecular mechanisms underlying this process are still not clear.

Reactive oxygen species (ROS), which act as second messenger and regulate the activity of various transcription factors, are both effectors of oxidative stress and potent triggers of inflammation. Several studies have indicated that an increased ROS level in myocardial tissue was associated with AF [8]. ROS-mediated activation of inflammatory signaling in cardiac tissues could lead to myocardial fibrosis while activation of transforming growth factor β1 (TGF-β1) could cause atrial structural remodeling. Interestingly, ROS was also found to act as a trigger of NLRP3 inflammasome activation. Similarly, angiotensin II (Ang II) was reported to regulate the generation of ROS in cells by activating membrane-bound NAD(P)H oxidase or inflammatory signaling [9]. Taken together, ROS may act as a bridge between NLRP3 activation and renin-angiotensin-aldosterone system (RAAS) activation in AF. Hence, we hypothesized that abnormal secretion of Ang II increased myocardial ROS generation and then activated the NLRP3 inflammasome, which induced cardiac myocytes' pyroptosis and activated inflammation in AF.

MicroRNAs (miRNAs) are small molecular RNAs composed of 19-25 nucleotides. They regulate target gene expression at the post-transcriptional level by acting on target mRNA and subsequently promoting the degradation of target mRNA or repressing target mRNA translation [10]. The effect of miRNAs in the pathogenesis of cardiac diseases such as arrhythmia, myocardial infarction and heart failure has been shown by many studies [11–13]. Still, only a few studies have focused on the role of miRNA mediated ROS regulation in AF. One study used right atrial tachypacing and found that overexpression of miR-206 induced ROS generation by negatively regulating SOD1 in the canine model of AF [14]. Another study reported exosomal miR-223 levels being significantly elevated after cardiopulmonary bypass, leading to downregulation of IL-6 and NLRP3 expression in the monocytes [15].

However, whether miR-223-3p could regulate Ang II-dependent ROS in AF via NLRP3 remains largely unknown. This study aimed to detect the correlation between oxidative stress and NLRP3 and explore the role of miR-223-3p in the injury of ROS induced by Ang II.

Material and methods

Tissue samples

The right atrial appendage (RAA) tissues were collected from patients with persistent (chronic) AF (cAF) who were undergoing open-heart surgery for coronary bypass grafting or valve replacement. The diagnosis of cAF is in accordance with the latest AHA/ASA guidelines. After tissue harvest, some of the samples were rapidly cryopreserved in liquid nitrogen and then stored at –80°C, until ready for use. The rest of the samples were washed with cool PBS and then fixed with 4% paraformaldehyde for fibrosis analysis. All patients included in the study were informed about the project and informed consent was received before the surgery. The experimental protocols were approved by the ethics committee of the first affiliated hospital of Guangxi Medical University.

Tissue fibrosis and malondialdehyde assay

To measure myocardial fibrosis, the fixed human atrial samples were imbedded in paraffin and serially sectioned into 4 μm thick slices for Masson's staining. To increase the statistical power, three fields of view for each slice were randomly selected and observed under an optical microscope (Olympus, Tokyo, Japan). Image-Pro 6.0 software was used to analyze the results. Malondialdehyde (MDA) levels were detected using the MDA kits (Nanjing Jiancheng Bioengineering Institute, Nanjing, China) according to the manufacturer's instructions.

Enzyme-linked immunosorbent assay

The serum Ang II levels were measured by a specific enzyme-linked immunosorbent assay (ELISA) kit (ab10601; Abcam, Cambridge, UK) according to the manufacturer's instructions.

Cell culture

We purchased the H9c2 cell line from the Chinese Academy of Sciences (Shanghai, China). After H9c2 cells were resuscitated, the cells were cultured in DMEM (10569010; Gibco, Gaithersburg, USA) with a proper volume of Penicillin-Streptomycin mix (15140148; Gibco, Gaithersburg, USA).

The incubator environment was adjusted to 37°C and 5% CO_2. Then cells were seeded in appropriate plates for the following experiments.

Cell Counting Kit-8 assay

We used a Cell Counting Kit-8 (CCK-8) assay (CK04; Dojindo, Kumamoto, Japan) to assess cell viability. Briefly, H9c2 cells were seeded in a 96-well plate and either incubated in different concentrations of Ang II (0 µm to 10 µm) (05-23-0101; Sigma, St. Louis, USA) for 24 h or incubated in Ang II for different lengths of time (from 0 h to 48 h). MCC950 is a potent specific inhibitor of the NLRP3 inflammasome and it blocks the release of IL-1β induced by NLRP3 activators such as lipopolysaccharide (LPS) and inflammatory factors. In the inhibitor group, MCC950 (50 µM) (HY12815; MedChem Express, Monmouth, USA) was added to the culture medium before stimulation with Ang II. After adding 10 µl of CCK-8 reagent into each well of the 96-well plate, the plate was incubated at 37°C for 2 h. Absorbance at 450 nm was then measured with the Varioskan Lux system (Thermo Fisher Scientific, Waltham, USA). The viability of the treated cells was measured according to the manufacturer's instructions. Experiments were performed at least in triplicate.

Transfection

After culturing for 24 h, all the cells were observed and evaluated under a microscope. Cells at 70–80% confluency in a 6-cell-culture dish were transfected with miR-223-3p mimics and miR-223-3p mimics negative control (NC) by Lipofectamine 3000 Reagent (Invitrogen, Carlsbad, USA). The sequences of the miR-223-3p mimics and NC used in the transfection experiment are listed in Table I. Both miR-223-3p mimics and miR-223-3p mimics NC were constructed by GenePharma (Shanghai, China). The transfection efficiency was determined by RT-qPCR. The transfected cells were cultured in serum-free medium for another 24 h and then treated with Ang II and MCC950 for further experiments.

Real-time quantification PCR analysis

Total RNA from the RAA tissues or harvested cells was extracted by Trizol (9108; Takara, Tokyo, Japan). cDNA was synthesized using a tailing reaction kit (B532451; Sangon Biotech, Shanghai, China) for miRNA or using a reverse transcription kit (RR047A; Takara, Tokyo, Japan) for mRNA. Subsequently, the cDNA was submitted to real-time quantification PCR (RT-qPCR) analysis on the StepOne System (Thermo Fisher Scientific, Waltham, USA), and quantified using the 2^{-CT} method with GAPDH used for normalization (for mRNA) or U6 (for miRNA). All primer sequences for RT-qPCR are listed in Table I.

Western blot analysis

The RAA tissues or harvested cells were lysed by RIPA lysis buffer (P0013B; Beyotime, Shanghai, China) with 1% PMSF (P0100; Solarbio, Beijing, China) and 1% phosphatase inhibitor (P1260; Solarbio, Beijing, China). The total protein concentration was measured with a BCA kit (P0012S; Beyotime, Shanghai, China). Each sample was mixed with 5 × SDS-PAGE loading buffer (P1040; Solarbio, Beijing, China) and subsequently boiled for 10 min at 100°C. Total protein (20 µg to 50 µg) was separated using SDS-PAGE electrophoresis and then transferred onto a PVDF membrane, followed by incubation in primary antibodies specific for NLRP3 (1:500, WL02635; Wanlei, Shenyang, China), ASC (1:750, sc-271054; Santa Cruz

Table I. Primers sequence for target genes

Subject		Primer
miR-223-3p	Forward	5'- TGTCAGTTTGTCAAATACC -3'
	Reverse	5'- AACTGGTGTCGTGAG -3'
U6	Forward	5'- CTCGCTTCGGCAGCACA -3'
	Reverse	5'- AACGCTTCACGAATTTGCGT -3'
NLRP3	Forward	5'- GTGGAGATCCTAGGTTTCTCTG -3'
	Reverse	5'- CAGGATCTCATTCTCTTGGATC -3'
GAPDH	Forward	5'- ACGGCAAGTTCAACGGCAC -3'
	Reverse	5'- CGCCAGTAGACTCCACGACATA -3'
miR-223-3p mimic	Sence	5'- UGUCAGUUUGUCAAAUACCCC -3'
	Antisence	5'- GGGGUAUUUGACAAACUGACA -3'
miR-223-3p mimic NC	Sence	5'- UUUGUACUACACAAAAGUACUG -3'
	Antisence	5'- CAGUACUUUUGUGUAGUACAAA -3'

miR – microRNA, NLRP3 – nucleotide-binding oligomerization domain-like receptor protein 3, GADPH – glyceraldehyde-3-phosphate dehydrogenase, NC – negative control.

Biotechnology, Santa Cruz, USA), caspase-1p20 (1:500, sc-398015; Santa Cruz Biotechnology, Santa Cruz , USA), IL-1β (1:500, ab2015; Abcam, Cambridge, UK), TGF-β1 (1:1000, ab179695; Abcam, Cambridge, UK), Col-1 (1:1000, ab96723; Abcam, Cambridge, UK) and GAPDH (1:10000, ab181602; Abcam, Cambridge, UK) at 4°C. Extra primary antibodies were washed. Then, membranes were incubated in secondary antibodies (1:10000, ab175773/ab150115; Abcam, Cambridge, UK) for 1 h at room temperature. An Odyssey Imaging System (LI-COR Biosciences, St. Charles, USA) was used to collect images of membranes.

ROS generation assay

Intracellular ROS level was measured by dichloro-dihydro fluorescein diacetate (DCFH-DA) (287810; Sigma, St. Louis, USA) according to the manufacturer's instructions. The fluorescence images were acquired by fluorescence microscopy (Olympus, Tokyo, Japan). Image-Pro 6.0 software was used to measure the average fluorescence intensity.

miR-223-3p target gene prediction

In order to find potential binding sites, we searched TargetScan (http://www.targetscan.org/) and miRbase (http://www.mirbase.org/) for target gene prediction of miR-223-3p. After prediction, the sequence of potential target genes with high scores was analyzed by the National Biotechnology Information Center BLAST program.

Dual luciferase assays

We generated a recombinant luciferase construct pSI-Check2-NLRP3 3′-UTR-WT (Promega, Madison, USA) harboring the fragments with the binding site for miR-223-3p and another recombinant construct pSI-Check2-NLRP3 3′-UTR-Mut with the mutated binding site for miR-223-3p. HEK293T cells were co-transfected with pSI-Check2-NLRP3 3′-UTR-WT recombinant plasmid (or pSI-Check2-NLRP3 3′-UTR-Mut recombinant plasmid) and miR-223-3p mimic (or miR-223-3p NC). Subsequently, dual-luciferase reporter assay was used to measure the luciferase activity in each group at 48 h after transfection.

Statistical analysis

In our article, the categorical data are presented as frequency and the continuous data are expressed as mean ± standard deviation (SD) or mean. The SPSS version 20 software was used for the statistical analysis. For categorical data, the differences between groups were compared by chi-square test. For continuous data, the difference in means between two groups with normally distributed data was compared using the two-tailed Student's *t*-test. In cases when there were more than two experimental groups, one-way ANOVA and the Holm-Sidak test were used for comparison. If the data were not normally distributed, the difference between groups was tested by Mann-Whitney and Kruskal-Wallis tests. The difference was considered statistically significant if the *p*-value was less than 0.05. Analyzed data were plotted as histograms using GraphPad Prism version 5 software.

Results

Baseline data of included patients

In total, 43 patients, including 20 patients with cAF, were enrolled. There was no significant difference in gender, age, disease composition, left ventricular ejection fraction and medicine therapy between the two groups ($p > 0.05$). The diameter of the left atrium in the cAF group was larger than that in the SR group (49.25 ±9.76 mm vs. 42.04 ±5.49 mm, $p = 0.004$). The baseline data summarizing the characteristics of included patients are listed in Table II.

Upregulation of NLRP3 inflammasome, fibrosis, and MDA expression in RAA of patients with cAF

To investigate the difference in NLRP3 inflammasome expression, fibrosis level and MDA level between SR and cAF patients, we examined the expression in RAA tissues from the two groups. Western blot results showed that in comparison to the SR group, the expression of NLRP3, ASC, caspase-1p20 and IL-1β was markedly higher in patients of the cAF group ($p < 0.05$) (Figure 1), suggesting enhanced activation of the NLRP3 inflammasome in patients with cAF. Masson's staining showed that the fibrosis level of RAA in the cAF group was significantly higher than that in the SR group (18.00 ±2.91% vs. 8.98 ±1.97, $p < 0.05$) (Figures 2 A, B). Meanwhile, western blot results demonstrated higher expression of Col-1 and TGF-β1 in the cAF group than that in the SR group (Figure 2 C). The result of the MDA test showed that the levels of MDA were markedly higher in the cAF group (5.378 ±1.067 nmol/ml vs. 3.544 ±1.052 nmol/ml, $p = 0.001$) (Figure 2 D).

Upregulation of serum Ang II level in patients with cAF

To investigate the serum Ang II level in patients with SR or cAF, the serum levels of Ang II were examined using a specific ELISA kit. As shown in Figure 2 E, the serum Ang II level was higher for

Table II. Baseline characteristics of included patients

Parameter	SR (n = 23)	AF (n = 20)	P-value
Gender (male/female)	11/12	7/13	0.395
Age [years]	57.00 ±8.37	55.85 ±7.88	0.647
Medical history:			
Coronary heart disease, n	8	9	0.494
Diabetes mellitus, n	7	6	0.975
Hypertension, n	5	7	0.334
Echocardiography:			
LAd [mm]	42.04 ±5.49	49.25 ±9.76	0.004**
LVEF (%)	58.35 ±9.94	56.75 ±8.25	0.573
Therapy:			
ACEI or ARB, n	14	11	0.697
β-blockers, n	8	7	0.988
Diuretics, n	3	5	0.440
Lipid-lowering medicine, n	8	9	0.494
Nitrates, n	3	4	0.687
Insulin, n	3	4	0.687

*SR – sinus rhythm as control, AF – atrial fibrillation, LAd – left atrial diameter, LVEF – left ventricular ejection fraction, ACEI – angiotensin converting enzyme inhibitors, ARB – angiotensin receptor blocker. *$p < 0.05$, **$p < 0.01$.*

patients with cAF than that in patients with SR (61.632 ±4.254 vs. 51.197 ±3.775, $p < 0.05$).

miR-223-3p expression level upregulated in patients with cAF

RT-qPCR results showed that the miR-223-3p expression in RAA was approximately three-fold higher in patients with cAF than that in the SR group (Figure 2 F).

Cell viability decreased notably after exposure to 1 μM Ang II for 24 h

To identify the effect of Ang II on cell viability, the H9c2 cells were stimulated with different concentrations of Ang II for different times. Compared with the control group, the cell viability gradually decreased first and then increased with increasing time and concentration. As shown in Figure 3 A, at a constant period of stimulation, the concentration of 1 μM of Ang II significantly decreased the H9c2 cell viability. Similarly, at constant stimulation concentration, the lowest cell viability was detected after Ang II exposure for 24 h (Figure 3 B). So, we used 1 μM Ang II for 24 h as an intervention condition for subsequent experiments.

miR-223-3p mimics downregulated the protein level of the NLRP3 inflammasome and ROS level induced by Ang II in H9c2 cells

To further explore the regulatory relationship between miR-223-3p and NLRP3, miR-223-3p mimics and miR-223-3p NC were transfected into H9c2 cells before intervention with Ang II. RT-qPCR results confirmed elevated levels of miR-223-3p in the mimic group (Figure 4 A). The protein expression of NLRP3 decreased in the mimic group (Figure 4 B). After intervention with Ang II, compared to the Ang II group, the protein expression of NLRP3, ASC, caspase-1p20 and IL-1β was markedly lower in the mimic group and Ang II + MCC950 group ($p < 0.05$) (Figure 4 C). The results of the ROS test showed that Ang II treatment promoted ROS generation in H9c2 cells. Meanwhile, the ROS level of the mimic group was lower compared with the Ang II group, while the same result was observed in the Ang II + MCC950 group ($p < 0.05$) (Figure 4 D). Intriguingly, cell viability was negatively correlated with ROS level in each group (Figure 4 E).

NLRP3 is the target gene of miR-223-3p

The results of bioinformatics analysis identified NLRP3 as a potential target gene of miR-223-3p with a conserved putative binding site between miR-223-3p and NLRP3 (Figure 5 A). In the dual-luciferase reporter assay, we found that compared with the NLRP3 WT + miR-223-3p NC group, (1) by the effect of miR-223-3p mimic, the luciferase activity of the NLRP3 WT + miR-223-3p mimic group was significantly lower (4.9664 ±2.0499 vs. 2.5562 ±0.7087, $p < 0.05$); (2) the decrease in luciferase activity was eliminated in the NLRP3 MUT + miR-223-3p mimic group and NLRP3 MUT+miR-223-3p NC group (Figures 5 B, C). These findings suggest

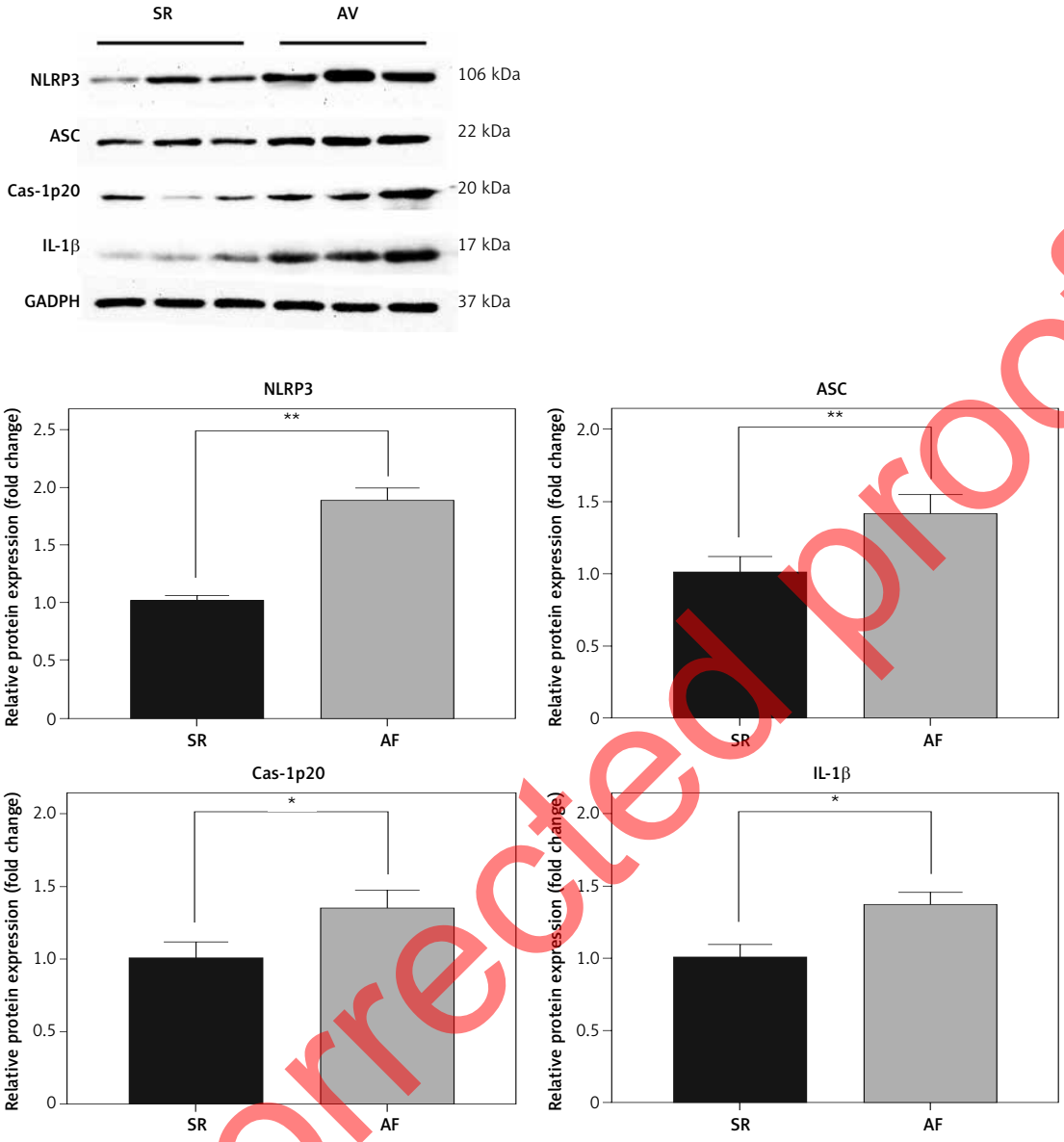

Figure 1. Enhanced activation of NLPR3 inflammatory signaling in RAA of patients with AF. Western blot analysis and quantification of NLRP3, ASC, caspase-1p20 and IL-1β. GAPDH was used as an internal control (n = 10)

**p < 0.05, **p < 0.01. GAPDH – glyceraldehyde-3-phosphate dehydrogenase, RAA – right atrial appendage.*

that when the predicted miR-223-3p binding site on the miR-223-3p 3′-UTR was mutated, binding of miR-223-3p to the NLRP3 3′-UTR was prevented. Taken together, these results confirmed that NLRP3 is a direct target gene of miR-223-3p.

Discussion

To date, several achievements have been made in AF catheter ablation treatment [16], yet the risk of AF continues to affect people's lives and increases with age. Increasing evidence suggests that oxidative stress and enhanced activation of NLRP3 inflammasome participate in the pathophysiological processes of AF. To our knowledge, activation of the NLRP3 inflammasome regulated by miRNAs in AF is not completely known. In the present study, we described the effect of miR-223-3p on regulation of the Ang II/ROS/NLRP3 axis in AF by targeting NLRP3. The schematic overview is shown in Figure 6.

Ang II is well known as an upstream regulatory factor that induces fibrosis in different organs. It is generally thought that abnormal secretion of Ang II directly mediates myocardial fibrosis by activating fibroblasts via AT1 targeting. Consistently with our study, Qiu *et al.* [17] reported a significantly elevated serum Ang II level in a chronic kidney disease rat model whose AF inducibility was significantly induced by transesophageal atrial burst pacing.

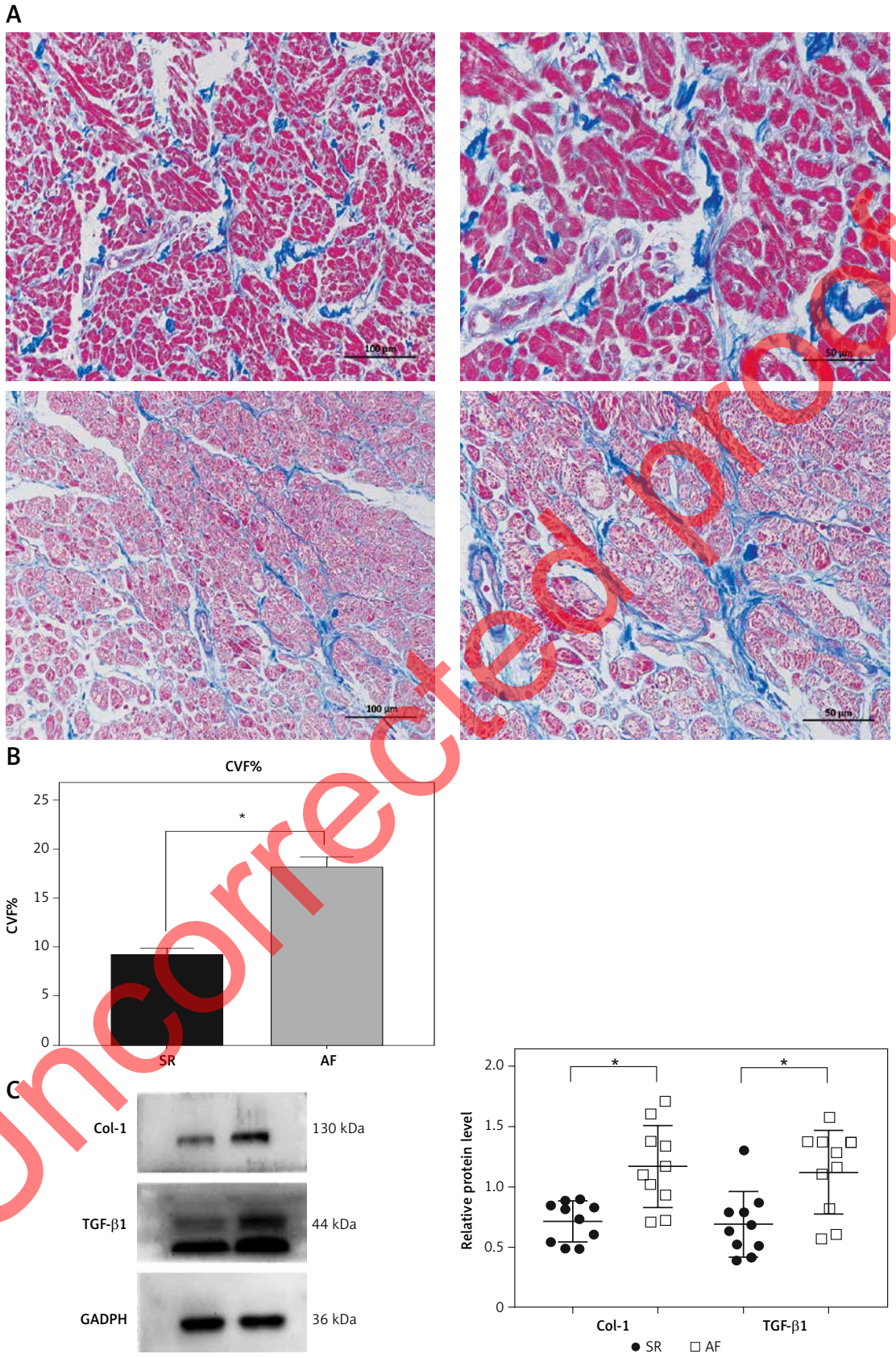

Figure 2. Increased fibrosis, MDA level, serum Ang II level and upregulated miR-223-3p in patients with AF. **A**, **B** – Masson's trichrome staining of RAA. The fibrosis area is blue. CVF was analyzed using Image-Pro 6.0 software (n = 6). **C** – Western blot analysis of Col-1 and TGF-β1 in RAA. GAPDH was used as an internal control (n = 10)

**p < 0.05, **p < 0.01. MDA – malondialdehyde, CVF – collagen volume fraction, ELISA – enzyme-linked immunosorbent assay, RAA – right atrial appendage, GAPDH – glyceraldehyde-3-phosphate dehydrogenase, miR – microRNA.*

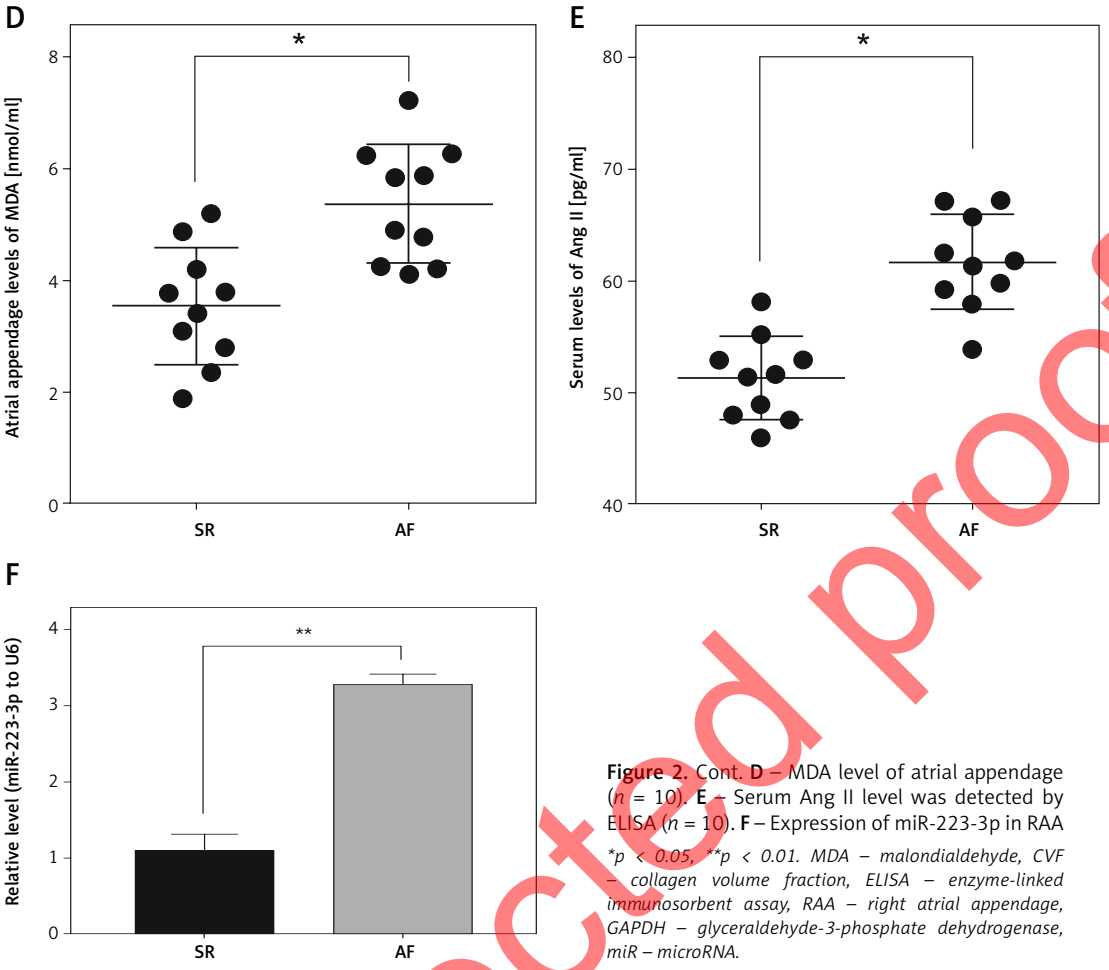

Figure 2. Cont. **D** – MDA level of atrial appendage (n = 10). **E** – Serum Ang II level was detected by ELISA (n = 10). **F** – Expression of miR-223-3p in RAA

**p < 0.05, **p < 0.01. MDA – malondialdehyde, CVF – collagen volume fraction, ELISA – enzyme-linked immunosorbent assay, RAA – right atrial appendage, GAPDH – glyceraldehyde-3-phosphate dehydrogenase, miR – microRNA.*

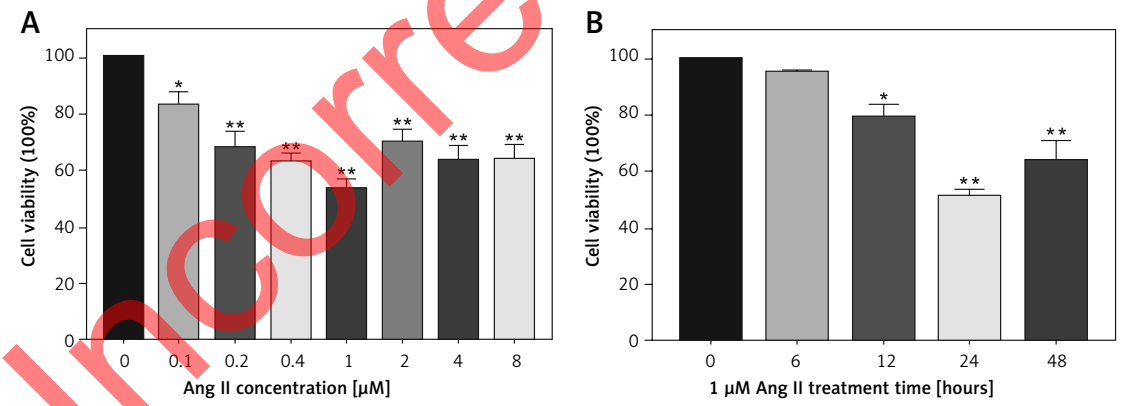

Figure 3. The impact of Ang II on cell viability. **A** – H9c2 cells were treated with different concentrations of Ang II and the cell viability was measured by CCK-8 assay. **B** – H9c2 cells were incubated with 1 μM Ang II from 0 h to 48 h (n = 3)

**p < 0.05, **p < 0.01; CCK-8 – Cell Counting Kit-8, RT-qPCR – real-time quantitative polymerase chain reaction.*

It is increasingly accepted that Ang II can induce a cardiac inflammatory response in atrial remodeling due to the notable expression of inflammatory genes at the early stage of Ang II infusion [18]. Furthermore, Epelman *et al.* [19] observed that recruitment of CCR2+ monocytes subsequently expanded to macrophages and pro-inflammatory cytokines were produced after Ang II intervention in the heart; however, this phenomenon could be inhibited by the CCR2 receptor. Hence, the inflammatory cytokines induced by Ang II could cause mitochondrial dysfunction and lead to the accumulation of ROS, which are recognized as potent endogenous damage-associated molecular patterns (DAMPs). In addition, the NLRP3 inflammasome could be activated by DAMPs.

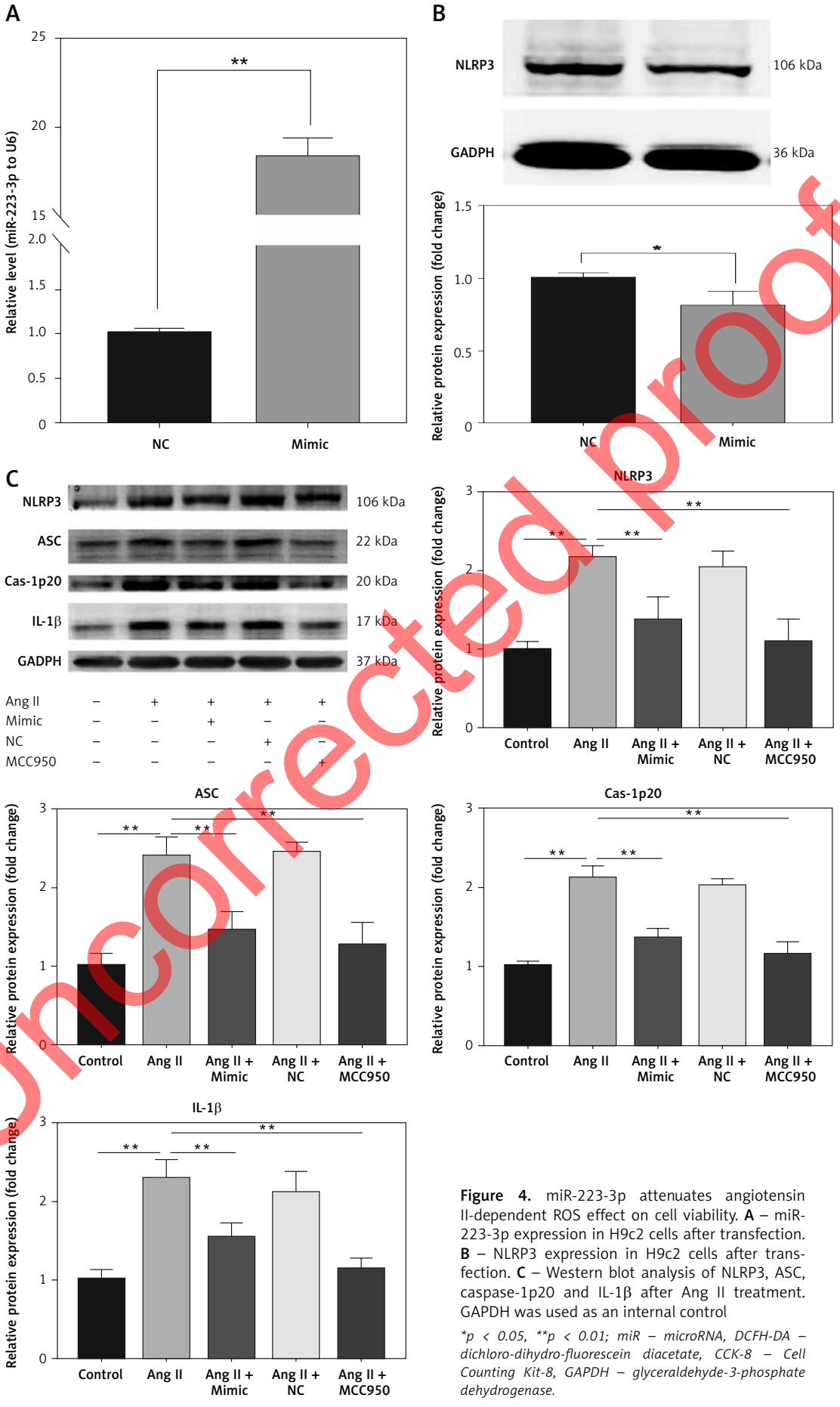

Figure 4. miR-223-3p attenuates angiotensin II-dependent ROS effect on cell viability. **A** – miR-223-3p expression in H9c2 cells after transfection. **B** – NLRP3 expression in H9c2 cells after transfection. **C** – Western blot analysis of NLRP3, ASC, caspase-1p20 and IL-1β after Ang II treatment. GAPDH was used as an internal control

**p < 0.05, **p < 0.01; miR – microRNA, DCFH-DA – dichloro-dihydro-fluorescein diacetate, CCK-8 – Cell Counting Kit-8, GAPDH – glyceraldehyde-3-phosphate dehydrogenase.*

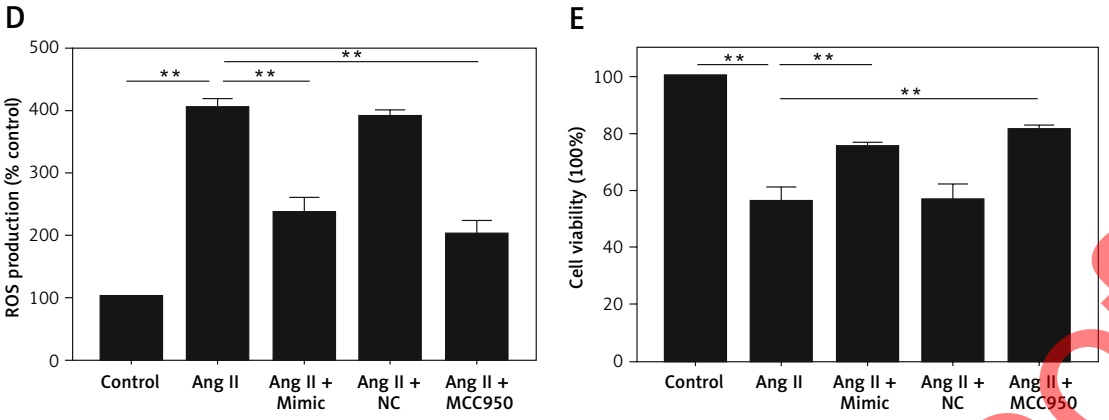

Figure 4. Cont. **D** – Intracellular ROS levels were measured by DCFH-DA. **E** – Cell viability was measured by CCK-8 assay (n = 6)

**p < 0.05, **p < 0.01; miR – microRNA, DCFH-DA – dichloro-dihydro-fluorescein diacetate, CCK-8 – Cell Counting Kit-8, GAPDH – glyceraldehyde-3-phosphate dehydrogenase.*

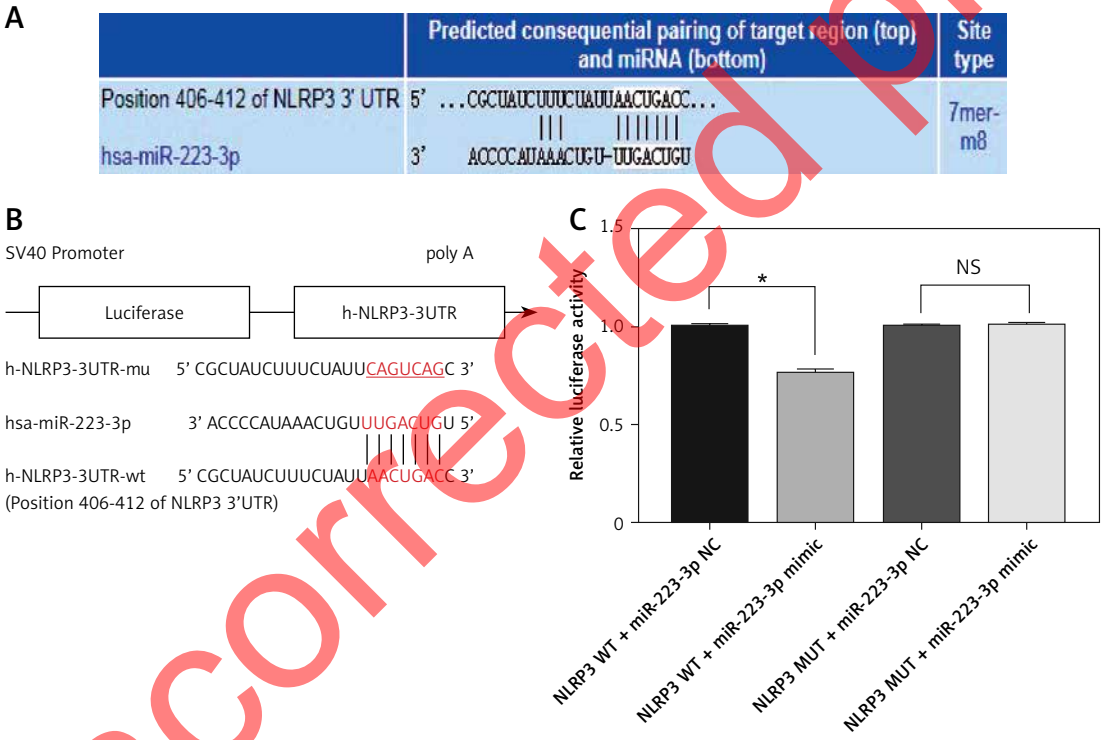

Figure 5. miR-223-3p targets NLRP3. **A** – Predicted site of miR-223-3p binding to NLRP3 mRNA in TargetScan. **B** – Schematic diagram of binding site between miR-223-3p and NLRP3-3'UTR target site. **C** – Wild type or mutant NLRP3 3'-UTR and miR-223-3p mimic or miR negative control were co-transfected into HEK 293 cells (n = 3)

**p < 0.05, **p < 0.01; miR – microRNA, UTR – untranslated region.*

Malondialdehyde and ROS are both classical detection indices for oxidative stress [20]. In recent years, several studies have suggested oxidative stress to be associated with AF [21, 22]. To better understand the role of oxidative stress in AF, we investigated MDA levels and found they were elevated in RAA of patients with cAF. For the *in vitro* study, we used Ang II to simulate a high circulatory Ang II level of AF and confirmed Ang II-mediated induction of ROS in H9c2 cells. Taken together, the above results emphasized that Ang II-mediated oxidative stress plays a crucial role in AF. In detail, oxidative stress is involved in the mechanism of AF in the following three aspects: atrial electrical remodeling, structural remodeling and connexin remodeling [23–26].

Ca^{2+}/calmodulin-dependent protein kinase II (CaMKII) is a serine threonine kinase and can be oxidized by ROS at methionine residues 281/282 and then transformed to ox-CaMKII, which is associated with cardiovascular disease [27]. Additionally, ox-CaMKII was identified as a proar-

rhythmic signal because of promoting delayed afterdepolarizations (DADs) in Ang II infusion [28]. This activation of CaMKII was also observed in cardiomyocytes after treatment of Ang II via the NADPH pathway [29]. To date, it has been found that CaMKII has four major isoforms (α, β, γ and δ), while CaMKIIδ is the mainly expressed isoform in the mammalian heart. Recently, non-ischemic stresses including Ang II were found to act as an activator of CaMKIIδ, which leads to cardiac inflammation. Willeford *et al.* [18] reported that after treatment of Ang II, the mRNA level of pro-inflammatory cytokines and the recruitment of macrophages decreased significantly in mice whose CaMKIIδ was genetically deleted. These results reveal that in Ang II mediated cardiac inflammation, the cardiomyocyte is the major site to elicit inflammation and activated CaMKIIδ plays an important role in Ang II induced inflammation. Moreover, Purohit *et al.* [28] identified CaMKII as an ROS sensor in the inflammatory response of Ang II signaling. The enhanced activation of CaMKII induced by ROS can in turn lead to mitochondrial dysfunction and more ROS induced by damaged mitochondria [30]. In other words, in Ang II signaling, CaMKII mediated ROS play a complementary role in the production of ROS induced by the NADPH pathway and expand the ROS effect on activation of the NLRP3 inflammasome. Thus, there is a mutual regulatory cycle between ROS production and CaMKII activation. CaMKII functions as a transducer of ROS production in Ang II mediating the inflammatory pathway.

Interleukin-1β, elevated in Ang II infusion, is a potent pro-inflammatory chemokine and could be generated through the NLRP3 inflammasome. In a clinical trial, Everett *et al.* [31] observed a significant decrease in risk of rehospitalization in patients with IL-1β signaling blocker treatment, suggesting that the NLRP3 inflammasome plays a crucial role in cardiac inflammation. In our study, we found enhanced activation of the NLRP3 inflammasome *in vivo* or *in vitro* by Ang II-independent ROS. Consistently with our study, Li *et al.* [32] found a significant increase in AF inducibility by constructing a CM-specific knock-in (CKI) mouse model which could express NLRP3. Conversely, the selective NLRP3 inflammasome inhibitor MCC950 could reduce the inducibility of AF in CKI mice [33]. So the activated NLRP3 inflammasome acts as an effector in the Ang II-dependent ROS-mediated inflammatory response.

The human NLRP3 gene is located in chromosome 1q44, which includes ten exons with a distribution of approximately 3.3 kb. The activated NLRP3 inflammasome plays an important role in pathogenesis of different diseases. Usually, the activated NLRP3 inflammasome signaling in cardiac

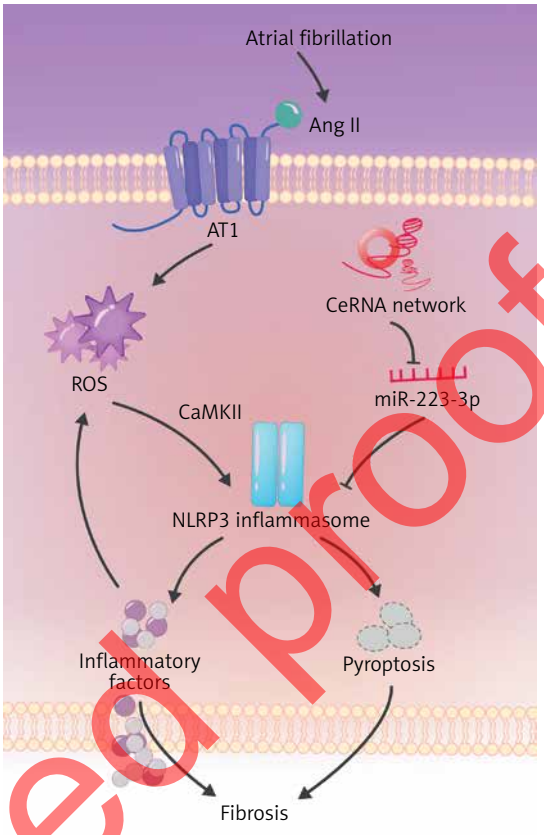

Figure 6. Schematic overview of current study

myocytes promotes the maturation of caspase-1 and then induces abundant release of mature IL-1β. IL-1β is known to be not only a profibrotic factor that is activated by TGF-β1 but also an important proinflammatory factor which could induce local or systemic inflammatory responses by promoting the expression of IL-6, TNF-α and CRP. In cardiac myocyte pyroptosis, abundant inflammatory mediators accumulate and cause cell edema. Under the action of perforin such as GSDMD [34], cell microchannels form and eventually induce cells pyroptosis, leading to the release of many inflammatory mediators. These mediators in turn activate inflammation via DAMPs and induce generation of more ROS, thereby aggravating myocardial damage. In the present study, Ang II increased the generation of ROS and subsequently activated NLRP3 inflammasome signaling, resulting in the release of inflammatory mediators, which in turn aggravated the downstream inflammatory cascades. As a result, inflammation mediated by inflammatory cytokines via DAMPs induced generation of more ROS, which in turn affected the cell viability.

A recent study reported that the exosomal miR-223 levels were significantly elevated after cardiopulmonary bypass, which led to downregulation of IL-6 and NLRP3 expression in the monocytes [15]. In order to detect the effects of miR-223-3p

in AF, H9c2 cells were transfected with miR-223-3p mimics before stimulation with Ang II. Compared with the NC group, NLRP3 expression was partly suppressed by miR-223-3p mimics. Interestingly, overexpression of miR-223-3p reduced the generation of Ang II induced ROS and inhibited the expression of the NLRP3/caspase-1/IL-1β axis. Meanwhile, the cell viability was partly attenuated in the miR-223-3p mimic group. Moreover, when cells were pretreated with MCC950 before stimulation, the NLRP3 expression and the generation of ROS were significantly reduced. MCC950, a potent selective inhibitor of NLRP3, can block NLRP3 activation. As discussed earlier, there is a mutual regulatory cycle between ROS production and CaMKII activation. After the cells were treated with MCC950, the effect of Ang II on enhanced NLRP3 activation was blocked, so the NLRP3 expression decreased compared with the Ang II group. The release of inflammatory cytokines decreased as well. As a result, the activation of CaMKII decreased due to mitochondrial damage decrease, which resulted in the decrease of ROS production. The above results indicated that miR-223-3p might function like MCC950 and negatively regulate NLRP3 inflammasome-mediated ROS generation, suggesting that the upregulated miR-223-3p plays a protective role in AF.

By using bioinformatics methods, NLRP3 was found to be a potential target gene of miR-223-3p. There was one predicted conserved binding site of miR-223-3p and NLRP3. Importantly, in the *in vitro* study we found a negative regulatory relationship between miR-223-3p and NLRP3. Furthermore, using a dual-luciferase reporter assay, we found that miR-223-3p could directly bind the 3′-UTR of NLRP3, thus confirming that NLRP3 is a direct target gene of miR-223-3p. Taken together, the evidence suggests that miR-223-3p may be involved in inhibiting activation of NLPR3 inflammasome signaling in AF by targeting NLRP3. However, the activation of NLRP3 was elevated in RAA as a result, which could partly be explained by the effect of miR-233-3p. MiR-223-3p was not strong enough to inhibit the NLRP3 expression to the level of patients without AF. Furthermore, *in vivo* the expression of NLRP3 may be affected by other mechanisms at the same time as the miRNA regulatory network is in many-to-many mode. An increasing number of studies have reported that a variety of long noncoding RNAs (lncRNAs) can weaken the effect of miRNAs on negatively regulating downstream gene expression by acting as competitive endogenous RNAs (ceRNAs). In detail, ceRNA can influence miRNA binding to the target gene by simulating molecular sponges, thus affecting the protein coding process. LncRNA growth inhibition specificity 5 (GAS5) is reported to play an important role in regulating vascular remodeling and acting as a tumor suppressor. Interestingly, a recent study reported that GAS5 functioned as a ceRNA and regulated hZIP1 expression by sponging miR-223-3p in renal cell carcinoma, whereas this effect was reversed by knockdown of GAS5 in an *in vitro* study [35]. However, Wang *et al.* [36] found that expression of miR-223-3p in patients with AF was decreased, which was different from our tissue experiment results. The difference may be due to the number of patients included and the influence of individual differences. Therefore, deeper studies on the role of miR-223-3p in AF pathophysiology need to be carried out in the future.

In conclusion, the oxidative stress induced by increased Ang II and activation of the NLRP3 inflammasome signaling pathway both play an important role in the process of AF. Upregulated miR-223-3p could partly attenuate the effect of Ang II-dependent ROS on cell viability by targeting NLRP3 in H9c2 cells. Therefore, the miR-223-3p and Ang II/ROS/NLRP3 inflammasome pathway may be a new valuable target for gene therapy of AF patients.

Acknowledgements

We would like to thank our teacher Dr. Zhong and everyone in our team for their hard work.

This work was supported by The Natural Science Foundation of China (NSFC) Grant (No. 81660054) and Guangxi Nova Program (No. 2016GXNSFBA380115) provided funds and technical support for this project. This study was also supported by the First Affiliated Hospital of Guangxi Medical University.

Conflict of interest

The authors declare no conflict of interest.

References

1. Chugh S S, Havmoeller R, Narayanan K, et al. Worldwide epidemiology of atrial fibrillation: A Global Burden of Disease 2010 Study. Circulation 2014; 129: 837-47.
2. Rahman F, Kwan G F, Benjamin EJ. Global epidemiology of atrial fibrillation. Nat Rev Cardiol 2014; 11: 639-54. Erratum in: Nat Rev Cardiol 2016; 13: 501.
3. Li B, Haridas B, Jackson AR, et al. Inflammation drives renal scarring in experimental pyelonephritis. Am J Physiol Renal Physiol 2017; 312: F43-53.
4. Song L, Pei L, Yao S, Wu Y, Shang Y. NLRP3 Inflammasome in- neurological diseases, from functions to therapies. Front Cell Neurosci 2017; 11: 63-79.
5. Xu Y J, Zheng L, Hu YW, Wang Q. Pyroptosis and its relationship to atherosclerosis. Clinica Chimica Acta 2018; 476: 28-37.
6. Strowig T, Henao-Mejia J, Elinav E, Flavell R. Inflammasomes in health and disease. Nature 2012; 481: 278-86.

7. Xu J, He Y, Luo B, et al. Correlation study between NLRP3 inflammasome and atrial fibrillation. Chinese Circulation Journal 2017; 32.
8. Yang Y, Zhao J, Qiu J, et al. Xanthine oxidase inhibitor allopurinol prevents oxidative stress-mediated atrial remodeling in alloxan-induced diabetes mellitus rabbits. J Am Heart Assoc 2018; 7: e008807.
9. Lu G, Xu S, Peng L, Huang Z, Wang Y, Gao X. Angiotensin II upregulates Kv1.5 expression through ROS-dependent transforming growth factor-beta1 and extracellular signal-regulated kinase 1/2 signalings in neonatal rat atrial myocytes. Biochem Biophys Res Commun 2014; 454: 410-6.
10. Farazi TA, Hoell JI, Morozov P, Tuschl T. MicroRNAs in human cancer. Adv Exp Med Biol 2013; 774: 1-20.
11. Rainer J, Meraviglia V, Blankenburg H, et al. The arrhythmogenic cardiomyopathy-specific coding and non-coding transcriptome in human cardiac stromal cells. BMC Genomics 2018; 19: 491.
12. Xue S, Liu D, Zhu W, et al. Circulating miR-17-5p, miR-126-5p and miR-145-3p are novel biomarkers for diagnosis of acute myocardial infarction [J]. Front Physiol 2019; 10: 123.
13. Dutka M, Bobinski R, Korbecki J. The relevance of microRNA in post-infarction left ventricular remodelling and heart failure. Heart Fail Rev 2019; 24: 575-86.
14. Zhang Y, Zheng S, Geng Y, et al. MicroRNA profiling of atrial fibrillation in canines: mir-206 modulates intrinsic cardiac autonomic nerve remodeling by regulating SOD1. PLoS One 2015; 10: e0122674.
15. Poon KS, Palanisamy K, Chang SS, et al. Plasma exosomal miR-223 expression regulates inflammatory responses during cardiac surgery with cardiopulmonary bypass. Sci Rep 2017; 7: 10807.
16. Demir GG, Güneş HM, Seker M, et al. Is the presence of left atrial diverticulum associated with recurrence in patients undergoing catheter ablation for atrial fibrillation? Arch Med Sci Atheroscler Dis 2019; 4: e25-e31.
17. Qiu H, Ji C, Liu W, et al. Chronic kidney disease increases atrial fibrillation inducibility: involvement of inflammation, atrial fibrosis, and connexins. Front Physiol 2018; 9: 1726.
18. Willeford A, Suetomi T, Nickle A, Hoffman HM, Miyamoto S, Brown JH. CaMKIIδ-mediated inflammatory gene expression and inflammasome activation in cardiomyocytes initiate inflammation and induce fibrosis. JCI Insight 2018; 3: e97054.
19. Epelman S, Lavine KJ, Beaudin AE, et al. Embryonic and adult-derived resident cardiac macrophages are maintained through distinct mechanisms at steady state and during inflammation. Immunity 2014; 40: 91-104.
20. Kaczmarczyk-Sedlak I, Folwarczna J, Sedlak L, et al. Effect of caffeine on biomarkers of oxidative stress in lenses of rats with streptozotocin-induced diabetes. Arch Med Sci 2019; 15: 1073-80.
21. Li YG, Chen FK, Deng L, et al. Febuxostat attenuates paroxysmal atrial fibrillation-induced regional endothelial dysfunction. Thromb Res 2017; 149: 17-24.
22. Leftheriotis DI, Fountoulaki KT, Flevari PG, et al. The predictive value of inflammatory and oxidative markers following the successful cardioversion of persistent lone atrial fibrillation. Int J Cardiol 2009; 135: 361-9.
23. Sovari AA. Cellular and molecular mechanisms of arrhythmia by oxidative stress. Cardiol Res Pract 2016; 2016: 9656078.
24. Kim N, Jung Y, Nam M, et al. Angiotensin II affects inflammation mechanisms via AMPK-related signaling pathways in HL-1 atrial myocytes. Sci Rep 2017; 7: 10328.
25. Jie L, Yu W, Xiaocui L, et al. Effect of oxidative stress on myocardial apoptosis, endoplasmic reticulum stress and apoptosis factor in suckling mouse atria myocardium. Zhongguo Ying Yong Sheng Li Xue Za Zhi 2017; 33: 185-8.
26. Petersen F, Rodrigo R, Richter M, Kostin S. The effects of polyunsaturated fatty acids and antioxidant vitamins on atrial oxidative stress, nitrotyrosine residues, and connexins following extracorporeal circulation in patients undergoing cardiac surgery. Mol Cell Biochem 2017; 433: 27-40.
27. Erickson JR, He BJ, Grumbach IM, Anderson ME. CaMKII in the cardiovascular system: sensing redox states. Physiol Rev 2011; 91: 889-915.
28. Purohit A, Rokita AG, Guan X, et al. Oxidized Ca2+/calmodulin-dependent protein kinase II triggers atrial fibrillation. Circulation 2013; 128: 1748-57.
29. Erickson JR, Joiner ML, Guan X, et al. A dynamic pathway for calcium-independent activation of CaMKII by methionine oxidation. Cell 2008; 133: 462-74.
30. Joiner ML, Koval OMa M, Li J, et al. CaMKII determines mitochondrial stress responses in heart. Nature 2012; 491: 269-73.
31. Everett BM, Cornel JH, Lainscak M, et al. Anti-inflammatory therapy with canakinumab for the prevention of hospitalization for heart failure. Circulation 2019; 139: 1289-99.
32. Li N, Scott L, Yao C, et al. Activation of NLRP3 inflammasome plays a role in the pathogenesis of atrial fibrillation. Heart Rhythm 2017; 14 (Suppl. 5).
33. Yao C, Veleva T, Scott L, et al. Enhanced cardiomyocyte NLRP3 inflammasome signaling promotes atrial fibrillation. Circulation 2018; 138: 2227-42.
34. Shi J, Zhao Y, Wang K, et al. Cleavage of GSDMD by inflammatory caspases determines pyroptotic cell death. Nature 2015; 526: 660-5.
35. Dong X, Kong C, Liu X, et al. GAS5 functions as a ceRNA to regulate hZIP1 expression by sponging miR-223 in clear cell renal cell carcinoma. Am J Cancer Res 2018; 8: 1414-26.
36. Wang Suyu, Min Jie, Yu Yue, et al. Differentially expressed miRNAs in circulating exosomes between atrial fibrillation and sinus rhythm. J Thorac Dis 2019; 11: 4337-48.